# Light-scattering studies of a ternary mixture: Comparison of field variables for critical phenomena description

D. L. Sidebottom and C. M. Sorensen
*Department of Physics, Kansas State University, Manhattan, Kansas 66506*

(Received 28 December 1987; accepted 21 April 1988)

We present static turbidity and dynamic light-scattering measurements near the critical double point of a mixture of secondary butyl alcohol, tertiary butyl alcohol, and water. At the critical double point of this mixture an upper two-phase miscibility loop merges with a lower two-phase region. When temperature is used as a field variable to describe the critical behavior of the turbidity and correlation length of the mixture, nonuniversal behavior is seen in both the critical exponents and amplitudes. If, however, the tBA concentration difference from the critical curve is used, universality is found in both exponents and amplitudes. We thus term this concentration difference to be the *relevant parameter* for proper description of the critical behavior and, following Griffiths and Wheeler [Phys. Rev. A 2, 1047 (1970)], show this relevant parameter was determined by it never having tangential paths of approach to the critical curve.

## I. INTRODUCTION

Over the past two decades considerable research has centered on investigation of critical phenomena which occur in liquid–gas systems and binary, ternary, and other multicomponent liquid systems.[1] An early consequence of these studies was the discovery that various thermodynamic quantities diverge whenever a critical point is encountered. The manner in which these divergences occur as the temperature of the system approaches the critical point (at $T = T_c$) has been shown to obey a power law of the form

$$A = A_0 t^{-a}, \tag{1}$$

where $t = |T - T_c|/T_c$, $a$ is the critical exponent, and $A_0$ is the critical amplitude.

Early studies revealed that systems composed of chemically different components shared the same set of critical exponents. Hence the critical exponents were said to be "universal." This principal of universality[2] can be understood in terms of the Ising model. This model revealed that the critical phenomena occurring near a phase transition are due largely to long-range correlations. The individual nature of how each particle interacts with its neighbor is overshadowed by these large scale interactions.

Not only were the exponents predicted to be universal, but particular relationships exist between different exponents that limit the number which need to be independently determined. These so-called scaling relations allow all the critical exponents to be determined once two are known. In a similar manner two-scale universality indicated that certain ratios formed from the amplitudes [$A_0$ in Eq. (1)] of particular diverging quantities were also universal.[3]

Binary systems typically can have only one critical point at atmospheric pressure. Ternary systems, however, typically have a locus of critical points formed by the presence of an extra concentration axis. Because of this locus of critical points, the coexistence surface of these ternary systems can often be complex. This, of course, is also true for a binary liquid in which the experimental convenience of constant atmospheric pressure is abandoned. Since the added dimensionality of these generalized systems provides a multitude of paths by which the critical point can be approached, Eq. (1) needs to be generalized to include field variables other than temperature.

Earlier work on ternary liquids or other mixtures which display complex coexistence behavior have shown interesting critical phenomena. In particular, exponent renormalization has been found when the critical point was approached along certain special paths. Studies of the coexistence curve,[4] correlation length,[5,6] susceptibility,[5,7] and shear viscosity[8] have all shown critical exponent doubling along paths which are asymptotically tangential or parallel to the critical curve. The general explanation of this exponent doubling can be obtained from Griffiths and Wheeler[9] who pointed out that a tangential approach to a critical curve will, in general, lead to modified critical exponents. The specific doubling nature of this modification was apparently described first by Griffiths in a private communication to Bartis and Hall[10] and is due to the asymptotically quadratic nature of the critical curve near an extremum necessary for a tangential approach. This convex, quadratic nature doubles the apparent exponent.

In this work we present light scattering data for a ternary system of tertiary butyl alcohol (2-methyl-2-propanol, hereafter referred to as tBA), secondary butyl alcohol (2-butanol, hereafter referred to as sBA), and water. By varying the ratio of the two alcohol isomers, a closed-loop coexistence region above another two-phase region can be formed.[11] The critical curve as a function of tBA concentration has two extrema at a hypercritical point and a critical double point. Our data were taken near the CDP where the upper closed loop can be made to merge with the lower two-phase region.

Our data involve both static turbidity and dynamic light-scattering measurements. The latter were used to determine the Rayleigh linewidth and to derive from there the fluctuation correlation length. We once again find exponent

 0021-9606/88/151608-08$02.10 

renormalization when temperature is used as a field variable. Near the CDP the exponents decrease rather than double due to the fact that our experiments here were performed on the concave side of the CDP.

We then show that when we use the tBA concentration as a field variable the exponents more nearly display their normal values. Our analysis also shows interesting results regarding the amplitudes of the divergence. Use of $T$ as a field variable does not allow for a universal description of all the data along different paths to the critical curve. Use of tBA concentration as the field variable, however, does lead to universal curves describing all the data regardless of the path of approach. We further amplify this idea by showing how the critical amplitudes along the $T$ and concentration directions are related by the slope of the critical curve.

Finally, we develop the idea proposed by Griffiths and Wheeler,[9] that the nontangential direction of concentration is the "*relevant*" direction having the "proper" amplitude and exponent. This relevancy is determined by the path's inability to ever be tangential to the critical curve. On the other hand, critical behavior along the possibly tangential temperature paths is slave to the relevant distance in concentration from the critical curve and the shape of the critical curve itself.

## II. EXPERIMENT

### A. Sample preparation and temperature control

For our light-scattering measurements to be reported here we prepared samples using water which was both distilled and deionized. The sBA used was Aldrich "Gold Label" and was 99.9% pure. The tBA used was reagent grade that was fractionally distilled in our laboratory.

The various mixtures used were formed volumetrically. We shall introduce the following nomenclature:

$V(\mathrm{w}), V(\mathrm{tBA}), V(\mathrm{sBA})$ = volume of water, tBA, sBA, respectively,

$V(\mathrm{BA}) = V(\mathrm{tBA}) + V(\mathrm{sBA})$ (i.e., volume of "butyl alcohol"),

$V(\mathrm{tot}) = V(\mathrm{BA}) + V(\mathrm{w})$ (i.e., total volume),

$x(\mathrm{tBA}) = V(\mathrm{tBA})/V(\mathrm{BA})$ and $x(\mathrm{BA}) = V(\mathrm{BA})/V(\mathrm{tot})$.

Stock solutions of butyl alcohol (BA) were produced at specific values of $x(\mathrm{tBA})$. Final samples were formed from these stock solutions and water by using a 1000 $\mu$l digital pippette. The pippette was accurate to within 10 $\mu$l hence the overall accuracy of $x(\mathrm{tBA})$ and $x(\mathrm{BA})$ was about 2%.

In order to measure turbidities ranging from about $3\times10^{-3}$ cm$^{-1}$ to around 1.0 cm$^{-1}$, two cells of differing path length were employed.

For large turbidities and photon correlation spectroscopy work, 4 ml samples were contained in 1 cm square borosilicate glass scattering cells. The square cells were 4.7 cm high and were fitted on top by a glass blower with a $\sim$20 cm long round glass tube 6 mm i.d. After filling, the contents were frozen in $LN_2$ and flame sealed with a torch at a point roughly 2/3 the way up the round glass tube. Pyrolysis of the samples was carefully avoided.

A doubly thermostated temperature control cell was constructed to maintain these samples at a fixed temperature. The rough temperature was achieved by circulating methanol from a temperature controlled circulator through copper coils attached to an outer brass can. Enclosed within and insulated from the outer can was a smaller inner brass can with an electrical heater. This inner can held the glass scattering cell. A precision thermistor placed in thermal contact with the sample was incorporated into a Kelvin bridge to determine the relative temperature. An additional thermistor and bridge circuit was used to control the heater current. This arrangement allowed us to obtain about 1 mK control of the temperature of the samples. Temperature changes of the samples were precise to about 0.2 mK. Thermal gradients along the length of the cell were reduced to less than 0.3 mK/cm.

For measurement of turbidities ranging from $3\times10^{-3}$ cm$^{-1}$ up to about 0.1 cm$^{-1}$ a cell with a 19.5 cm path length was employed. This long cell was constructed from a 20 mm i.d. glass tube with windows attached at each end perpendicular to the axis of the tube. The temperature was maintained by a surrounding glass jacket fed by the circulating bath. The temperature of this bath was stable over hourly operation to about 0.02 °C. Unfortunately, the temperature of the sample itself was not easily obtained and was uncertain by about 0.5 °C. This is not a serious deficiency since turbidities in this range only occur far from the critical point where the turbidity is a slow function of $T$.

The experiments were performed on six different mixtures. These mixture were: mixture 10$U$, $x(\mathrm{tBA}) = 10\%$, $x(\mathrm{BA}) = 46.3\%$; mixture 10$L$, $x(\mathrm{tBA}) = 10\%$, $x(\mathrm{BA}) = 49.0\%$; mixture 15$U$, $x(\mathrm{tBA}) = 15\%$, $x(\mathrm{BA}) = 45.0\%$; mixture 15$L$, $x(\mathrm{tBA}) = 15\%$, $x(\mathrm{BA}) = 48.5\%$; mixture 25$U$, $x(\mathrm{tBA}) = 25\%$, $x(\mathrm{BA}) = 44.3\%$; and mixture 25$L$, $x(\mathrm{tBA}) = 25\%$, $x(\mathrm{BA}) = 50.0\%$. The tBA concentrations were chosen to explore the system both near and far from the CDP along both the upper "$U$" (high $T$) and lower "$L$" (low $T$) branches of the critical curve. The BA concentrations were chosen to be close to the critical BA isopleths at the six different critical points. Photon correlation measurements were not successful in the 25$L$ sample due to large viscosities and subsequent correlation times too long for us to accurately measure. These paths of approach, as well as the general features of the coexistence behavior of the $BA/H_2O$ system, are shown in Figs. 1 and 2. The curves in Fig. 1 represent cloud point measurements and thus are strictly speaking not coexistence curves. The dashed line in Fig. 1 and the solid line in Fig. 2 do, however, accurately describe the critical curve.

The location of each critical point was determined by observing the behavior of several samples, near their separation temperature, whose compositions encompassed the actual critical composition. The relative volume of each phase was measured when a sample attained equilibrium just inside the two-phase regime ($\Delta T\sim0.1$ °C) after having been agitated. The critical composition is that which when agitated, just inside the two-phase region, separates into equal volumes upon reaching equilibrium.[12] Details of the determination of these curves and the critical curve itself are given elsewhere.[11]

Experimental problems such as wetting effects, impuri-

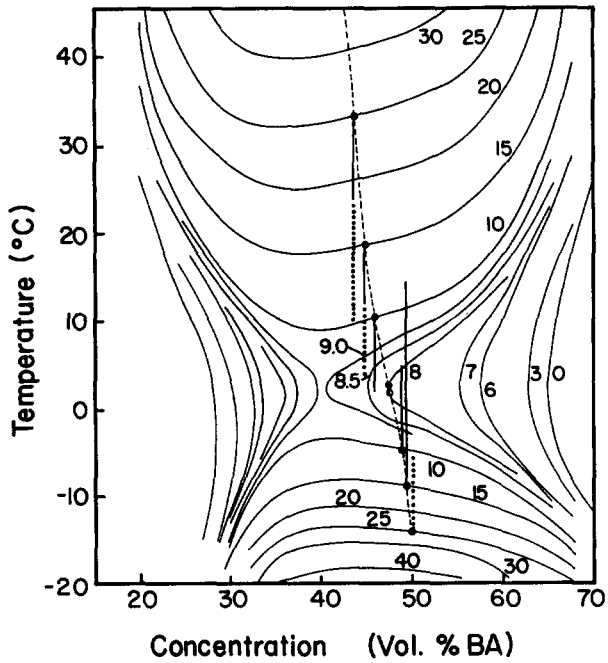


FIG. 1. Cloud point curves for the mixture of tBA, sBA, and water. BA concentration is the total volume percentage of tBA plus sBA in the solution. Different curves are for different tBA fractions, $x$(tBA). Dashed line is the critical curve. Solid vertical lines are the paths over which both turbidity and dynamic light-scattering data were obtained, dotted lines are paths over which only turbidity data were taken. tBA concentrations of these paths are given by $x$(tBA) where they terminate on a cloud point curve.

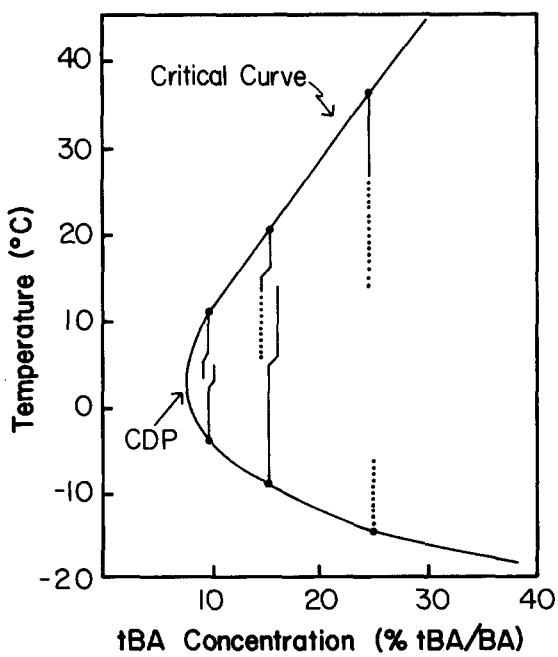


FIG. 2. Critical curve as a function of tBA concentration $x$(tBA) vs temperature. The one-phase region is to the right of the critical curve. CDP is the critical double point. As in Fig. 1, solid vertical lines are the paths over which both turbidity and dynamic light-scattering data were obtained, dotted lines are paths over which only turbidity data were taken. For clarity these lines are offset in regions of overlap.

ties, or gravity induced density gradients were either minimized or irrelevant. No wetting effects were seen. Impurities were avoided as described above. Their unsuspected presence could modify the absolute position of the coexistence surface, but the conclusions drawn in this work depend solely upon relative location of the critical curve with respect to the path of approach taken. Hence small impurity amounts have no effect on our results. Giglio *et al.*[13] have shown that gravity induced concentration gradients are not significant for times scales of the experiment except when very near to the critical point ($\Delta T \lesssim 100$ mK). As a precaution, samples were periodically shaken between measurements. Also the beam passed through the center of the sample to within 5%.

### B. Photon correlation spectroscopy

Photon correlation spectroscopy (PCS) was performed to determine the correlation length of the concentration fluctuations that were present in the samples near the critical point. This technique measures the lifetime of concentration fluctuations occurring in the sample by measuring the intensity autocorrelation function of quasielastically scattered light at a fixed angle from the sample.[14] The optical arrangement included a laser source that was focused by a lens to about 100 $\mu$ diameter beam waist as it passed through the sample. Light scattered from the sample at 31° was refracted by the walls of the 1 cm square cell and collected at an external angle of 45°. An image of the scattering volume was focused by a collection lens onto a pinhole located about 50 cm ahead of the cathode of a photomultiplier tube. This arrangement provided sufficient spacial coherence of the light impinging upon the cathode to produce an acceptable signal-to-noise ratio. A slit was used here to block out unwanted light and ensure homodyne detection. The output signal from the PMT was amplified and digitized and fed to a commercial correlator which computed the correlation function.

The correlation function was comprised of 64 channels, the first 56 of which were sequential, the last 8 were delayed. The correlation function obtained was fit to an exponential that included two cumulants and a background:

$$\langle I(0)I(t)\rangle = B + A\exp(-\mu_1 t - \tfrac{1}{2}\mu_2 t^2 + \cdots), \quad (2)$$

where $I$ is the instantaneous scattered intensity and the brackets indicate an ensemble average. $\mu_1$ is the first cumulant and is related to the linewidth by $\mu_1 = 2\Gamma$. The background $B$ represents the average of the square of the scattered intensity and was determined from counts obtained in the last eight channels at the far end of the spectrum ($t > 5\mu_1^{-1}$). Fits were judged by both their "chi-square" values (a statistical measure of the goodness of the fit) as well as the relative smallness of the second cumulant ($\mu_2/\mu_1^2$) which should be zero.

Viscosities necessary to determine correlation lengths from the PCS linewidths were determined by using Poiseuille flow viscometers in temperature controlled baths.

### C. Turbidity

The turbidity $\tau$ of any substance is defined by the Beer–Lambert law

$$I_t = I_0 e^{-\tau l}, \tag{3}$$

where $I_t$ and $I_0$ are the transmitted and incident intensities, respectively, and $l$ is the length of the path traversed by the light through the substance.

For measurement of turbidities of about $5\times10^{-2}$ cm$^{-1}$ and larger, the 1 cm square cells that were used to obtain the PCS results were also used. The laser source was divided by a beam splitter and the reflected portion was monitored by a reference photodiode while the rest of the light was attenuated by the sample before arriving at the second photodiode. The photocurrent produced was converted to voltage and amplified. A ratio of the two voltages derived from the photodiodes was obtained from a slide-wire potentiometer. The potentiometer provided the ratio $V_1/V_2$ to about 1%. This voltage ratio is related to $I_t/I_0$ through a constant that accounts for various instrumental corrections, such as cell wall reflections, beam splitter, and the different characteristics of the two photodiode/amplifier circuits. In each case this constant was determined later by calibrating these short cell results to the long cell turbidities which were absolute.

Measurements of turbidities in the range $3\times10^{-3}$ to 0.1 cm$^{-1}$ were obtained using the long path cell. Early work with this long cell indicated that problems with the alignment of the beam through the cell were negligible and that only one photodiode was needed. Hence corrections for a beam splitter and for electrical characteristics of the amplifiers were nonexistent in this situation. The ratios of $I_t/I_0$ could be found by physically removing and replacing the cell into the beam, and measuring the resulting voltages with a quality voltmeter. No beam splitter was involved and measurements were made within a time frame small enough that intensity variations of the laser would not affect the results.

The loss of intensity due to reflections at the windows was determined by studying the transmission of several common simple fluids whose vertically polarized Rayleigh ratios at 25 °C were known. The turbidity is directly related to the Rayleigh ratio[15] and is typically $10^{-5}$ cm$^{-1}$. This is small enough to be negligible so that the loss of light in the cell was due solely to the window interfaces. In this way we found that each window of our long cell had a transmittance of $0.93\pm0.03$. By accounting for the losses due to the windows, the long cell afforded us a direct measurement of the turbidity of the samples.

## III. DATA ANALYSIS

The PCS light scattering data were analyzed by relating the measured first cumulant of the scattering light correlation function, Eq. (2), to the mutual diffusion coefficient $D$ of the BA and water system

$$\mu_1 = 2Dq^2, \tag{4}$$

where $q$ is the scattering wave number given by

$$q = \frac{4\pi n}{\lambda}\sin\theta/2. \tag{5}$$

Here $n$ is the refractive index of the solution and $\theta$ is the scattering angle. The refractive index of our solutions was $n = 1.37$.

Inversion of Eq. (4) yields the diffusion coefficient $D$ which will have both a background and a critical part,

$$D = D_B + D_C. \tag{6}$$

Current results indicate that the critical part[16] is well described by

$$D_C = \frac{Rk_BT}{6\pi\eta\xi}\Omega_K(q\xi), \tag{7}$$

where $k_B$ is Boltzmann's constant and $R$ is a factor close to unity. We shall take $R = 1.0$. The Kawasaki function $\Omega_K(q\xi)$ is given by[17]

$$\Omega_K(x) = \frac{3}{4x^4}[1 + x^2 + (x^3 - x^{-1})\arctan x]. \tag{8}$$

The background part is given by[18,19]

$$D_B = \frac{k_BT}{16\eta_0\xi}\left[\frac{1+q^2\xi^2}{q_c\xi}\right], \tag{9}$$

where $\eta_0$ is the coefficient of the viscosity divergence and $q_c$ is a cutoff wave number.[20]

Our task was to determine the correlation length $\xi$ from the experimentally determined first cumulant $\mu_1$ and viscosity $\eta$ and Eqs. (4)–(9) above. The sensitivity of $\mu_1$ to $\xi$ is limited by the large $x$ form of the Kawasaki function, Eq. (8). When $q\xi \geqslant 1$, $\mu_1$ becomes relatively insensitive to $\xi$. Thus values of $\xi > q^{-1}$ were not used in the analysis.

The major problem in the extraction of $\xi$ is the uncertainty in the background term. The viscosity $\eta$ has a weak divergence and our data were in the range $|T - T_c| \geqslant 30$ mK so that $\eta \simeq \eta_0$ is a good approximation. The wave vector $q_c$, which essentially determines the magnitude of the background, is unknown. We analyzed our data for $q_c = \infty$ (i.e., no background) and for a few values down to $q_c = 6\times10^6$ cm$^{-1}$, which yielded the largest background. This range of backgrounds was picked from examination of $q_c$ values obtained in other binary and ternary liquid systems.[6,21] Double logarithmic graphs of the correlation lengths vs $T - T_c$ determined from the data for this variety of $q_c$'s all showed the same slopes, hence same critical exponents, $\nu$, within experimental error for each solution studied. Furthermore, the small multiplicative factors between $\xi$ values for different $q_c$ values were essentially the same for all solutions. Thus, we found in this range of $q_c$ that the effect of $q_c$ was to systematically alter $\xi$ by at most 40%. Our approach was to pick an "average" or "most reasonable" $q_c$, which we picked to be $10^7$ cm$^{-1}$ and then used this in our subsequent analysis. Our $\xi$ values might within reason have $\pm$ 20% systematic error but no error is incurred in the critical exponents or intercomparisons between different solutions which is the primary purpose of this work.

Our turbidity data were obtained using both $Ar^+$ and He–Ne lasers operating at $\lambda = 5145$ or 6328 Å, respectively. This occurred because a considerable amount of data had been obtained at 5145 Å when the laser died. This forced us to use the He–Ne laser. Because of this and our desire to display all the turbidity data in a comparative manner, we corrected the 5145 Å data to 6328 Å by a wavelength to the fourth power correction. For $T - T_c < 100$ mK a more subtle and complex correction is also needed, but we found this

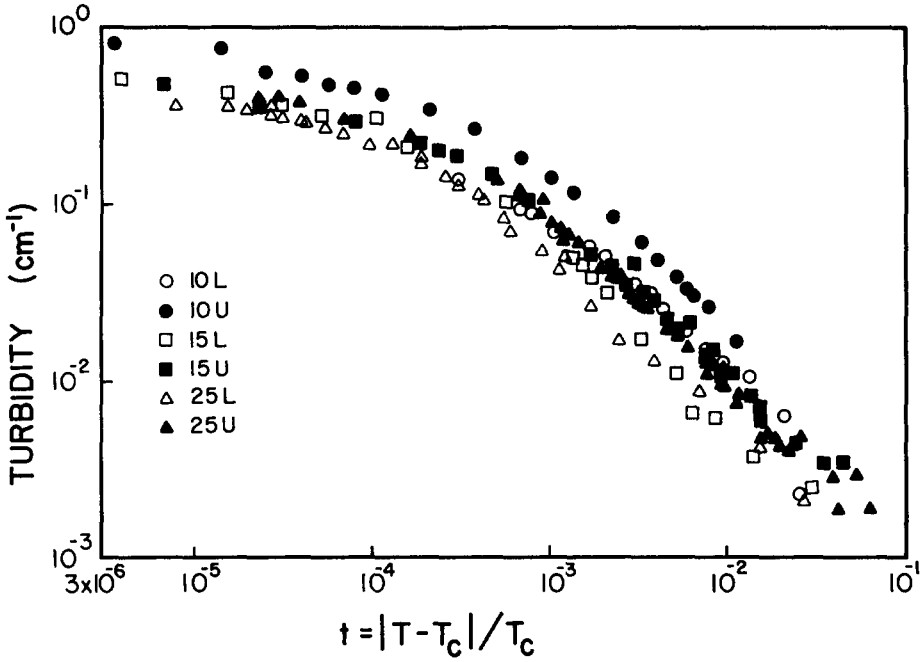


FIG. 3. Turbidity as a function of reduced temperatures for the six solutions studied.

correction to be much smaller than our experimental error and thus did not apply it.

## IV. RESULTS

The turbidity data vs reduced temperature, $t = |T - T_c| T_c^{-1}$, are displayed in Fig. 3. These data are qualitatively similar to turbidity measurements in binary liquid systems. In our system different solutions representing different $x$(tBA) and either upper or lower critical points show the same critical behavior, as indicated by the similar slopes at larger $t$ and subsequent rounding off of $\tau$ in the same region of smaller $t$.

Differences appear, however, in the amplitudes of the critical behavior in $\tau$. The turbidity is expected to obey[22]

$$\tau = \tau_0 \Gamma t^{-\gamma} f(a), \tag{10}$$

where

$$a = 2(k_0 \xi)^2 \tag{11}$$

and

$$f(a) = (2a^2 + 2a + 1)a^{-3} \ln(1 + 2a) - 2(1 + a)a^{-2}. \tag{12}$$

$k_0$ is the incident wave number $2\pi/\lambda$. Thus the differences between the six solutions lies in $\tau_0 \Gamma$. $\tau_0$ is dependent on the chemical makeup of the system, which given the isomerism of tBA and sBA, implies $\tau_0$ is most likely nearly constant in

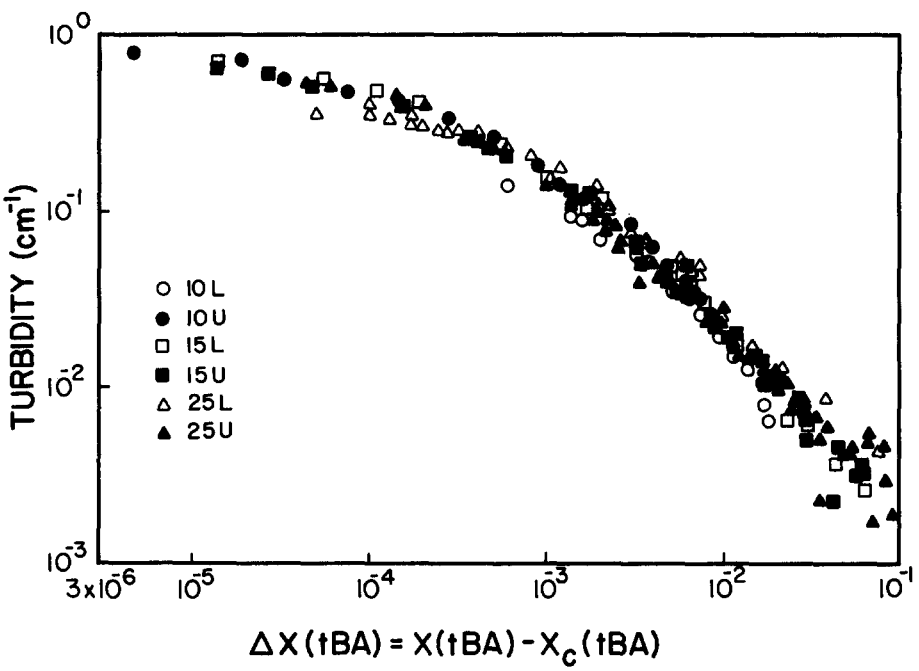


FIG. 4. Turbidity as a function of tBA concentration difference from the critical curve $\Delta x(\text{tBA}) = x(\text{tBA}) - x_c(\text{tBA})$.

the six solutions. Thus it seems the critical amplitude of the susceptibility $\Gamma$ varies from solution to solution when $t$ is the field variable.

Given the complex nature of the phase diagram as indicated by the cloud point measurement results shown in Figs. 1 and 2, $t$ is not the only possible choice for a field variable to describe the critical phenomena of this system. If we make a quasibinary assumption, $x(\text{tBA})$ can also be used as a field variable. It is important to stress that a field variable is one which has equal values in both coexisting phases. This is probably not exactly true for $x(\text{tBA})$. A quasibinary assumption would entail using Figs. 1 and 2 as coexistence curves rather than cloud point curves. Thus the lines of constant $x(\text{tBA})$ in Fig. 1 would represent coexistence curves describing coexisting phases with equal $x(\text{tBA})$. That this approximation is at least somewhat reasonable was demonstrated in an earlier analysis of the cloud point curves under this assumption[11] when compared to similar curves in sBA/$H_2O$ systems in which the field variable pressure was used.[23]

To use $x(\text{tBA})$ as a field variable we plot in Fig. 4 $\tau$ vs $\Delta x(\text{tBA}) = x(\text{tBA}) - x_c(\text{tBA})$ where $x_c(\text{tBA})$ is the tBA concentration at the critical point. To understand the construction of $\Delta x(\text{tBA})$, refer to Fig. 2. Given a temperature $T$ along any of the six iso-$x(\text{tBA})$ paths of approach, a corresponding $x_c(\text{tBA})$ can be found by going to the left in Fig. 2 at constant $T$ until the critical curve is encountered. $\Delta x(\text{tBA})$ is just the length of this isothermal line. Although the absolute uncertainty in the composition of a given sample is $\sim 2\%$, the value of $\Delta x(\text{tBA})$ near the critical point can be more accurately determined. Since the location of the critical point is known to $\leqslant 10$ mK and the slope of the critical curve can, at that point, be estimated to within a few percent, the precision in $\Delta x(\text{tBA})$ is roughly $10^{-5}$. In Fig. 4 we see that all the turbidity data collapse to one universal curve within experimental error when plotted vs $\Delta x(\text{tBA})$. Comparison of Figs. 3 and 4 graphically demonstrates the superiority of $\Delta x(\text{tBA})$ over $t$ and to some extent vindicates our pseudobinary assumption. We would claim that $\Delta x(\text{tBA})$ is the *relevant parameter* to describe the critical properties of $\tau$.

In terms of the critical amplitude $\Gamma$, Fig. 3 shows that $\Gamma$ is different for different solutions when $t$ is the field variable, whereas Fig. 4 shows that $\Gamma$ is equal for all solutions when $\Delta x(\text{tBA})$ is the field variable.

Similar but more detailed behavior is seen for the correlation length $\xi$ determined from the PCS measurements. Figure 5 shows $\xi$ vs $t$ for five solutions. One solution, 15$L$, stands away from the rest, indicating a different critical amplitude. The increase in $\xi$ for $t > 4\times 10^{-2}$ in this solution is due to the closer approach to the upper critical point at $x(\text{tBA}) = 15\%$ as we drew further away from the lower critical point (see Fig. 2). The 10$L$ solution has a slope significantly less than the others. The 10$U$ solution also shows a somewhat smaller slope. The results of least-squares fits to the linear portions of these curves using

$$\xi = \xi_0^{(t)} t^{-\nu} \tag{13}$$

are given in Table I. The fits have limited precision because the log–log plots in Fig. 5 are not particularly linear. All solutions show exponents $\nu$ below the expected Ising value of $\nu = 0.63$[1]. The smallest values of $\nu$ are found for both $x(\text{tBA}) = 10\%$ solutions. For these solutions, at least, we believe this renormalization to smaller values can be understood as due to the concave curvature of the critical curve near $x(\text{tBA}) = 10\%$ as compared to the renormalization of exponents to larger values (exponent doubling) as has been observed near convex critical curves.[4–8]

Figure 6 shows the correlation length data plotted against $\Delta x(\text{tBA})$. In contrast to the behavior of $\xi$ vs $t$ we once again find all the data collapse to a single curve. In this case both slopes (exponents) and amplitudes are modified from the variant $t$ dependence to the unified $\Delta x(\text{tBA})$ dependencies.

We now fit the correlation length data to

$$\xi = \xi_0^{(x)} \Delta x(\text{tBA})^{-\nu}. \tag{14}$$

The results are also given in Table I. Here we see the wide variation in amplitudes and exponents present in the fit with $t$ as the field variable, Eq. (13), is gone. The amplitudes and exponents are all nearly equal within experimental error. This is as expected from the behavior displayed in Fig. 6. Puzzling, however, is the fact that the exponents $\nu$ are all small compared to the expected value of $\nu = 0.63$. This discrepancy is most likely due to our pseudobinary assumption; i.e., we expect that $\Delta x(\text{tBA})$ is only an approximation to a

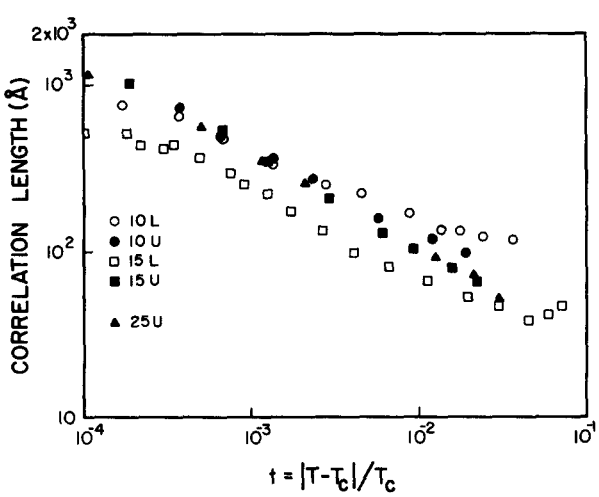


FIG. 5. Correlation length as a function of reduced temperature for five of the six solutions studied.

TABLE I. Fit parameters to Eq. (13) or (14) for the correlation length. Individual errors in the amplitudes and exponents are roughly ± 15% and ± 6%, respectively.

| Solution | $\xi_0^{(t)}$ (Å) | $\nu$ | $\xi_0^{(x)}$ (Å) | $\nu$ |
|---|---|---|---|---|
| 10$L$ | 21 | 0.42 | 12 | 0.55 |
| 10$U$ | 12 | 0.51 | 13 | 0.54 |
| 15$L$ | 5 | 0.56 | 9 | 0.59 |
| 15$U$ | 7 | 0.60 | 8 | 0.62 |
| 25$U$ | 8 | 0.56 | 11 | 0.57 |

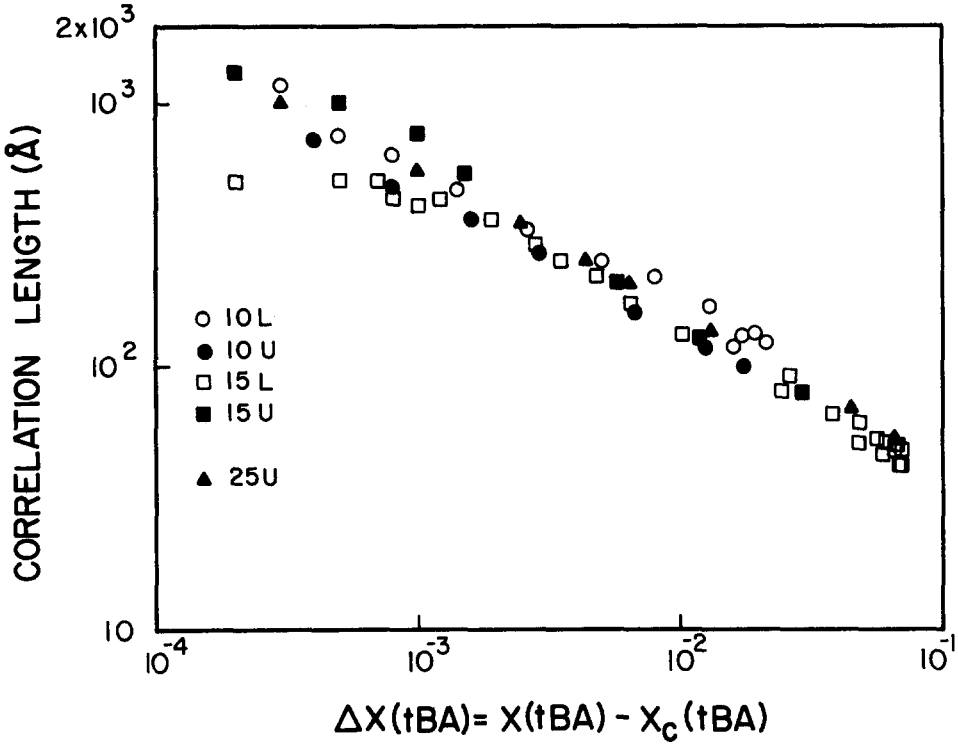


FIG. 6. Correlation length as a function of tBA concentration difference from the critical curve $\Delta x(\mathrm{tBA}) = x(\mathrm{tBA}) - x_c(\mathrm{tBA})$.

true field variable. If $\Delta x(\mathrm{tBA})$ and the correct concentration field variable were related in a slightly nonlinear way, then a slight renormalization of the exponents could result. We can only speculate that this is so. This does not deter us from the conclusion that $\Delta x(\mathrm{tBA})$ is a good approximation to the concentration field variable and that description of the critical phenomena in terms of this field variable yields a universal description in both amplitudes and exponents.

It is interesting to point out that the parameter $\Delta x(\mathrm{tBA}) = x(\mathrm{tBA}) - x_c(\mathrm{tBA})$ is not a reduced parameter. At first thought it would seem that the proper description would be obtained with the reduced parameter $\tilde{x}(\mathrm{tBA}) = \Delta x(\mathrm{tBA})/x_c(\mathrm{tBA})$ in analogy to the reduced temperature $t$. Graphs of $\tau$ or $\xi$ vs $\tilde{x}(\mathrm{tBA})$ were nearly as deviant from solution to solution as the $t$ graphs but more disordered. Empirically, $\Delta x(\mathrm{tBA})$, as shown in Figs. 4 and 6, is far superior. We point out that $\Delta x(\mathrm{tBA})$ is unitless so no units problem arises in its use.

An interesting relationship concerning the critical amplitudes of the correlation length $\xi_0$ can now be derived by comparison of the $t$ and $\Delta x(\mathrm{tBA})$ directions on the phase diagram. If we ignore the $10U$ and $10L$ data in Fig. 5, we see that the $15U$ and $25U$ data fall on nearly the same curve, whereas the $15L$ data are parallel but at lower values by a factor of roughly 1.5. This was reflected in the least squares results for $\xi_0^{(t)}$ and $\nu$ for these solutions given in Table I, where $\nu$ is essentially the same for all three, but $\xi_0^{(t)}$ for $15L$ is smaller by a factor of 1.5 (again) than the other two.

If indeed $\Delta x(\mathrm{tBA})$ is the relevant parameter to describe critical phenomena in this system, the difference in critical amplitudes using $t$ as the field variable can be understood in terms of different slopes of the critical curve in the $x(\mathrm{tBA})$–$T$ plane. Figure 2 shows that the critical curve is fairly linear near the critical points of all three of these solutions. The slopes of the upper curve at 15% and 25% tBA are nearly the same but distinctly different than the slope of the lower curve near 15% tBA.

These different slopes yield different critical amplitudes when $t$ is used as the field variable. To understand this consider the schematic diagram in Fig. 7. Drawn here is an $x$–$t$ plane of field variables, which in our case represent concentration and temperature, but could be any two field variables. Also drawn is a linear critical curve with slope $m$. If $x$ is the *relevant parameter* then the divergence of a given property, for our example the correlation length, is given by

$$\xi = \xi_0^{(x)} x^{-\nu}, \tag{15}$$

where $\xi_0^{(x)}$ represents the amplitude when $x$ is used as the

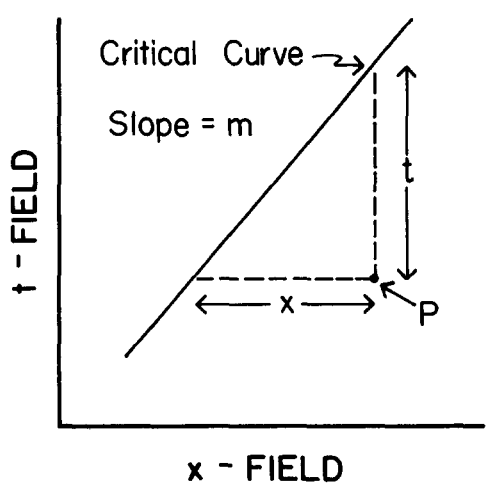


FIG. 7. Schematic of a linear critical curve as a function of reduced field variables $x$ and $t$.

field variable. To describe how $\xi$ depends on $t$ we use the slope of the critical curve. Thus

$$t = mx, \tag{16}$$

so that

$$\xi = \xi_0^{(x)} m^{-\nu} t^{-\nu} = \xi_0^{(t)} t^{-\nu}. \tag{17}$$

This shows that the two critical amplitudes $\xi_0^{(x)}$ and $\xi_0^{(t)}$ are related by the slope and that for a linear critical curve the exponent is unchanged. In our system the critical curve has two linear regions of different slope. Since $x$(tBA) was the relevant parameter, $\xi_0^{(x)}$ does not change, but $\xi_0^{(t)} = m^{\nu} \xi_0^{(x)}$ will with $m$. One then finds for the upper and lower critical curves that

$$\frac{\xi_0^{(t)}(\text{upper})}{\xi_0^{(t)}(\text{lower})} = \left(\frac{m(\text{upper})}{m(\text{lower})}\right)^{\nu}. \tag{18}$$

From Fig. 2 we find the slope ratio to be 2.0 which raised to the $\nu = 0.6$ power is 1.5. From Table I we find the amplitude ratio to be 1.5 in good agreement with the slope ratio calculation. This argument once again demonstrates that $\Delta x$(tBA) is the relevant parameter for describing the critical phenomena of this liquid mixture and that the reduced temperature merely tags along in obedience.

## V. CONCLUSIONS

We have found nonuniversal behavior in the critical behavior of our light-scattering data when temperature is used as the field variable. This nonuniversal behavior was displayed in both the critical exponents and amplitudes being functions of the path of approach. On the other hand, if tBA concentration was used as the field variable, universality was regained in *both* the critical exponents and amplitudes which were independent of the approach path.

The geometric picture of critical phenomena due to Griffiths and Wheeler may be used to explain these results. To use this picture we recognize that the approach to the critical curve when temperature is a field variable can be tangential to the critical curve. Thus, this field variable is singled out by nature as a special case in which modified exponents may result. These modified exponents occur in regions where the critical curve is not linear, usually near paths of approach that are tangential to the critical curve. Our data also show that the critical amplitudes may also vary between paths. In contrast to the exponents, these amplitudes are modified even along paths that are not tangential to the critical curve. All that is necessary is that this field variable path be tangential to the critical curve *at some point* in phase diagram, not necessarily the particular path of study. On the other hand, tBA concentration paths in our system appeared never to be tangential to the critical curve and hence should display universal behavior. This is what we observed with both constant exponents and amplitudes for all paths. Lack of experimental agreement of exponent values with the Ising value (experiment was $\sim 10\%$ too small) was probably due to the imperfectness of $\Delta x$ as a field variable for our system. Despite this, we can conclude that in describing the critical phenomena in our system the tBA concentration $x$(tBA) is the *relevant parameter*, a term we have used above to stress its nature.

In summary, the critical phenomena near a critical curve are universally described by a relevant field variable determined by the condition that no path of variation of this field variable be tangential to the critical curve. Any field variable which is at some point tangential to the critical curve is enslaved by the relevant parameter and the shape of the critical curve for determination of critical exponents and amplitudes as this field is varied.

## ACKNOWLEDGMENTS

This work was supported by NSF Grant Nos. CHE-8219571 and CHE-8618576.

[1] J. V. Sengers and J. M. H. Levelt Sengers, in *Progress in Liquid Physics*, edited by C. A. Croxton (Wiley, New York, 1978), p. 103.
[2] L. P. Kadanoff, in *Critical Phenomena*, edited by M. S. Green (Academic, New York, 1971).
[3] D. Stauffer, M. Ferer, and M. Wortis, Phys. Rev. Lett. **29**, 345 (1972).
[4] S. Deerenberg, J. A. Schouten, and N. J. Trappeniers, Physica **103**, 183 (1980).
[5] R. G. Johnston, N. A. Clark, P. Wiltzius, and D. S. Cannell, Phys. Rev. Lett. **54**, 49 (1985).
[6] C. M. Sorensen and G. A. Larsen, J. Chem. Phys. **83**, 1835 (1985).
[7] R. J. Tufeu, P. H. Keyes, and W. B. Daniels, Phys. Rev. Lett. **35**, 1004 (1975).
[8] G. A. Larsen and C. M. Sorensen, Phys. Rev. Lett. **54**, 343 (1985).
[9] R. B. Griffiths and J. C. Wheeler, Phys. Rev. A **2**, 1047 (1970).
[10] J. T. Bartis and C. K. Hall, Physica A **78**, 1 (1974).
[11] C. M. Sorensen (to be published).
[12] D. Beysens, in *Phase Transitions*, edited by M. Levy, J.-C. Le Guillou, and J. Zinn-Justin (Plenum, New York, 1982), p. 25.
[13] M. Giglio and A. Vendramini, Phys. Rev. Lett. **35**, 168 (1975).
[14] B. J. Berne and R. Pecora, *Dynamic Light Scattering* (Wiley, New York, 1976).
[15] M. Kerker, *The Scattering of Light and Other Electromagnetic Radiation* (Academic, New York, 1969).
[16] H. C. Burstyn and J. V. Sengers, Phys. Rev. A **25**, 448 (1982).
[17] K. Kawasaki, in *Phase Transitions and Critical Phenomena*, edited by C. Domb and M. S. Green (Academic, New York, 1978), Vol. 5a, p. 165.
[18] D. W. Oxtoby and W. M. Gelbart, J. Chem. Phys. **61**, 2957 (1974).
[19] J. K. Bhattacharjee, R. A. Ferrell, R. S. Basu, and J. V. Sengers, Phys. Rev. A **24**, 1469 (1981).
[20] T. Ohta, J. Phys. C **10**, 791 (1977).
[21] D. L. Henry, L. E. Evans, and R. Kobayashi, J. Chem. Phys. **66**, 1802 (1977).
[22] V. G. Puglielli and N. C. Ford, Jr., Phys. Rev. Lett. **25**, 143 (1970).
[23] T. Moriyoshi, S. Kaneshina, K. Aihara, and K. Yabumoto, J. Chem. Thermodyn. **7**, 537 (1975).